PARTICLE BACKSCATTER AND EXTINCTION PROFILING WITH THE SPACEBORNE HSR DOPPLER WIND LIDAR ALADIN

Albert Ansmann(1), Paul Ingmann(2), Olivier Le Rille(2), Dulce Lajas(2), and Ulla Wandinger(1)

(1) *Leibniz Institute for Tropospheric Research, Permoserstr. 15, 04318 Leipzig, Germany, E-mail: albert@tropos.de, ulla@tropos.de*

(2) *European Space Research and Technology Centre, Keplerlaan 1, 2201 AZ Noordwijk, The Netherlands, E-mail: paul.ingmann@esa.int, olivier.lerille@esa.int, dulce.lajas@esa.int*

ABSTRACT

The potential of ALADIN to measure the optical properties of aerosol and clouds is investigated based on end–to–end simulation studies. A comprehensive data analysis scheme is developed and briefly presented here. The error analysis shows that the particle backscatter and extinction coefficients, and the corresponding extinction–to–backscatter ratio can be obtained with an overall (systematic and statistical) error of 5%–10% (backscatter) and 10%–30% (extinction, lidar ratio) in the polluted boundary layer (700 shots, 500–m vertical signal resolution), and 10%–20% (backscatter) and 20%–40% (extinction, lidar ratio) in cirrus (140 shots, 1000 m resolution). The data sets generated with ALADIN are expected to be included in a long–term data base consisting of observations of optical properties of aerosols and clouds provided by missions like CALIPSO, ADM–Aeolus, and EarthCARE.

1. INTRODUCTION

The Atmospheric Dynamics Mission (ADM [1]) is an approved mission of the European Space Agency with a target date of launch in 2008. The primary aim of ADM–Aeolus is to provide global observations of wind profiles. The high–spectral–resolution Doppler lidar ALADIN (Atmospheric Laser Doppler Lidar Instrument [2]) carried by Aeolus (named after *the keeper of the winds* in Greek mythology) will permit the retrieval of line–of–sight wind velocity profiles. ALADIN is a direct–detection wind lidar capable of using the backscatter signal from both molecular (Rayleigh) and aerosol (particle) scattering to retrieve independent wind information. ALADIN will be the most powerful spaceborne lidar ever launched (Table 1). The signal strength will be almost a factor of 50 stronger than the signal of the CALIPSO lidar.

A schematic view of the ALADIN measurement geometry is shown in Figure 1. ALADIN emits laser pulses at a wavelength of 355 nm towards the atmosphere. The backscattered lidar returns are analyzed to determine the shift of the frequency with respect to the outgoing laser pulse frequency caused by spacecraft motion and wind velocity (and Earth rotation). As shown in Figure 1, the lidar measures the wind projection along the laser beam (line of sight, LOS), using a slant angle versus nadir of 35°. The lidar beam is pointed perpendicular to the flight track to avoid contamination by horizontal spacecraft motion (about 7 km/s).

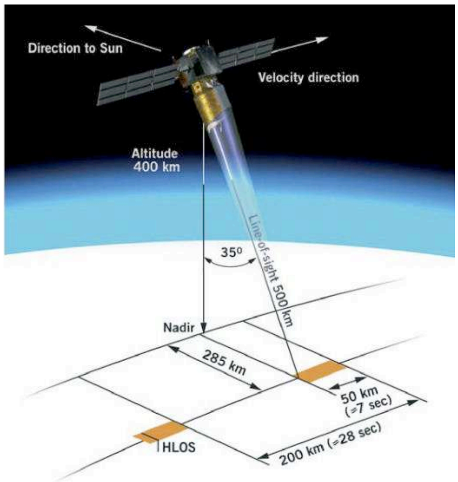

Figure 1: Schematic view of the ALADIN measurement geometry. ALADIN is operated in the so–called burst mode, i.e., 700 shots are transmitted within 50 km during a 7–second period (shaded areas, horizontal line of sight HLOS). During the remaining 21 seconds of the 28–second cycle no observations will be taken. The laser will be switched off for about 10 seconds.

Figure 2 illustrates the three ALADIN backscatter detection channels. From these signals independent information of the frequency shift and thus on the

Table 1: ALADIN parameters

Lidar altitude	408 km
Lidar wavelength	355 nm
Laser pulse energy	120 mJ
Pulse repetition rate	100 Hz
Primary mirror diameter	1.5 m
Vertical resolution	250 m – 2000 m

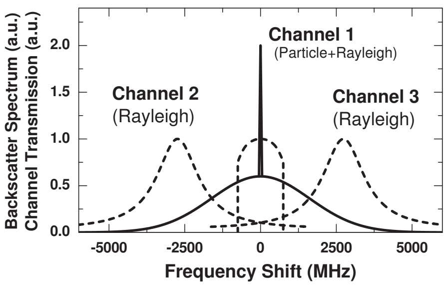

Figure 2: Spectral profiles of particle (Mie peak) and Rayleigh backscattering (broad spectrum, solid curve) and of the transmission functions (dashed curves) of the central channel 1 (Fizeau interferometer, idealized curve) and of the channels 2 and 3 (double–edge Fabry Perot etalon).

LOS velocity can be retrieved. Figure 2 shows the case for zero LOS velocity. For 50 m/s the backscatter spectrum is shifted by about 300 MHz.

ALADIN will be the first high–spectral–resolution lidar (HSRL) in space and thus will also allow a global mapping of aerosol and cloud (cirrus) optical properties [3]. These data are expected to be included in a long–term data base (2006–2014) consisting of observations of optical properties of aerosols and clouds provided by missions like CALIPSO, ADM–Aeolus, and EarthCARE.

The potential to derive simultaneously wind and aerosol optical properties at 355 nm was recently demonstrated [4,5]. Here, we show an alternative way. After a careful cross–talk correction of the measured Rayleigh signals, we use the well–established Raman lidar approach to compute backscatter and extinction profiles [6].

2. DATA ANALYSIS SCHEME

Three methods are available to determine aerosol and cloud optical properties from the three ALADIN signal profiles (cf. Table 2). The HSRL extinction and backscatter techniques (or the respective Raman lidar procedures as preferred here) allow an independent retrieval of the particle backscatter and extinction coefficients. The HSRL methods are robust and can be regarded as the backbone of the entire data analysis. The third method, the Klett method, is rather uncertain because of the sensitive influence of the 355–nm lidar–ratio input on the backscatter solutions. This is in particular the case when the forward mode of the Klett method is used to retrieve lower–tropospheric backscatter profiles from spaceborne lidar data [7,8].

Table 2: Data analysis procedure

(1)	Rayleigh signal correction (I) Cross–talk correction (Fig.3, top) (II) Frequency shift correction (Fig.3, center) (III) Temp.-broadening correction (Fig.3, bottom)
(2)	Cross–talk correction check (compare Klett and HSRL solutions in cirrus)
(3)	HSRL backscatter retrieval (Raman lidar approach [6])
(4)	HSRL extinction retrieval (Raman lidar approach [6])
(5)	Klett backscatter retrieval [7,8]

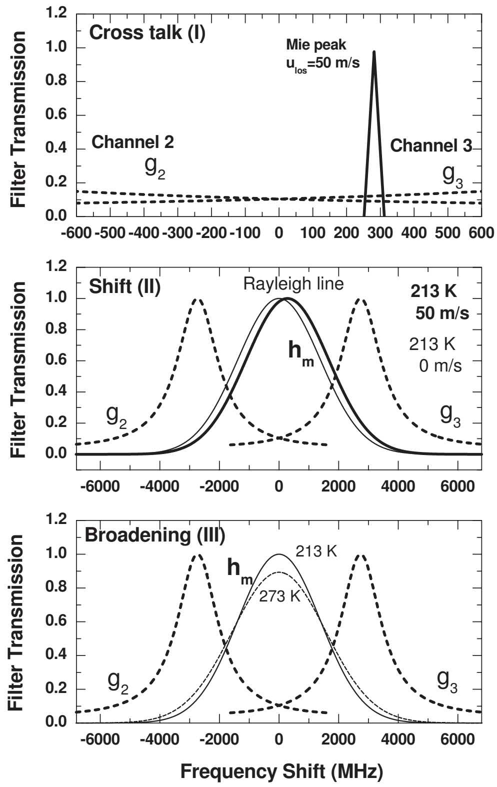

Figure 3: Rayleigh signal correction procedure: Step (I) Cross–talk correction, step (II) correction of the velocity–induced Doppler shift of the Rayleigh line, step (III) correction of temperature–dependent Rayleigh line broadening. g_2 and g_3 describe the transmission profiles of the Rayleigh channels 2 and 3. The Rayleigh backscatter spectrum is described by h_m.

Before the aerosol retrieval methods can be applied to the ALADIN observations, three different corrections must be applied to the range– and background–corrected molecular signal profiles (Rayleigh channels 2 and 3, cf. Table 2). The corrections are illustrated in Figure 3. A very accurate cross–talk correction, i.e., the removal of the signal contribution caused by particle backscattering from the Rayleigh signals, is a fundamental requirement for a successful retrieval of particle optical properties by using the HSRL method. The cross–talk correction is done by the use of the channel–1 signals.

In the second step, the impact of the LOS–velocity–induced shift of the Rayleigh backscatter spectrum on the Rayleigh signals is removed. The backscatter spectrum is shifted back (to obtain the spectrum for zero velocity) for each height layer resolved with ALADIN. For the case shown in Figure 3 (center plot) the correction of the shift effect leads to an increase of the Rayleigh signal 2 and a decrease of the Rayleigh signal 3. The signals are afterwards normalized to zero velocity.

Similarly, in the third step, the influence of temperature broadening of the Rayleigh backscatter line on the Rayleigh signals is corrected. The signals are normalized to 273–K backscatter conditions. As illustrated in Figure 3, the channels 2 and 3 detect more backscattered light at 273 K than at 213 K (for zero velocity). Accordingly, the Rayleigh signals measured at temperatures $T < 273$ are increased. However, the corrections (II) and (III) are of minor importance.

The central channel (Fizeau interferometer, Figure 2) detects the central part of the Rayleigh spectrum only (from −750 to 750 MHz) and thus only 32% (at 273 K) to 40% (at 190 K) of the total Rayleigh backscatter. This effect has to be considered in the HSRL and Klett backscatter procedures.

In order to check the quality of the cross–talk correction we compare the optimum Klett solution (backward mode solution = forward mode solution) with the respective HSRL backscatter profile in an isolated cirrus cloud in the upper aerosol–free troposphere. In contrast to the HSRL results, the Klett solutions do not suffer from cross–talk effects. We adjust one of the lidar input parameters that sensitively influence the cross–talk correction such that the Klett and HSRL solution almost coincide. Based on a large set of simulations for very different cases with simple and complex aerosol and cirrus layering we can conclude that this method guarantees a high–quality removal of the cross–talk effect and subsequently a high–quality retrieval of the optical properties of all relevant aerosol and cirrus layers in the troposphere and stratosphere.

After a proper, quality–checked Rayleigh signal correction, we finally can apply well–established retrieval methods [6] to derived particle backscatter and extinction profiles from simultaneously measured aerosol signals and pure molecular signals (here the sum of the two cross–talk–corrected Rayleigh signals).

3. SIMULATIONS

Two ALADIN simulations are shown in Figures 4 and 5. 140 shots (10 km horizontal resolution, Figure 4) and 700 shots (50 km resolution, Figure 5) are averaged. Strong LOS–velocity variations with

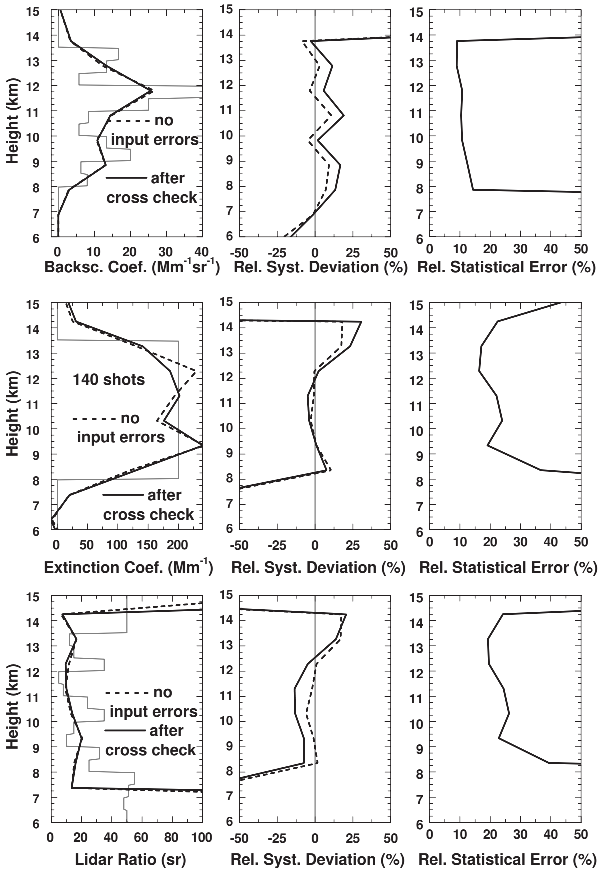

Figure 4: Nighttime observations (140 shot average) of particle optical properties with ALADIN (HSRL method). No errors in the atmospheric and lidar system parameters are simulated in the case of the dashed curves. The solid curves are obtained by simulating realistic errors in all input parameters and after applying the quality check of cross–talk correction. Systematic deviations of the retrieved solutions from the respective input values used in the ALADIN signal simulation are shown. Statistical errors are caused by signal noise. Thin gray curves (left) show the true backscatter and extinction profiles with 50–m range resolution (as used in the basic signal simulation from which the low–resolution ALADIN signals are then calculated).

height, from 20–60 m/s in the cirrus in Figure 4 and 20–35 m/s in the lower troposphere in Figure 5, are simulated.

As can be seen in Figure 4, a good retrieval of particle optical properties in cirrus is possible. The particle backscatter and extinction coefficients, and the corresponding extinction–to–backscatter ratio can be obtained with an overall (systematic and statistical) error of 10%–20%, 20%–30%, and 20%–40%, respectively. The simulations showed no significant difference between daytime and nighttime performance. An additional error of the order of 10% (desert dust) to 20% (clouds) must be kept in mind in the interpretation of backscatter and lidar ratio profiles because ALADIN detects the parallel–polarized component of backscattered light (backscattered at 35° nadir

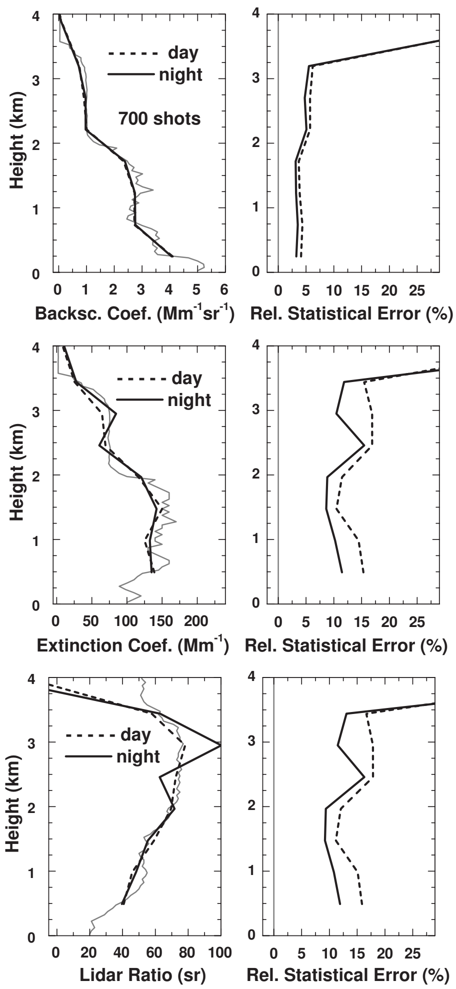

Figure 5: Particle backscatter and extinction coefficients, extinction–to–backscatter ratio, and corresponding statistical uncertainties for 700–shot averages and nighttime (solid curves) and bright daytime conditions (dashed curves). Thin gray curves (left) show the true backscatter and extinction profiles with 50–m range resolution (as used in the signal simulation).

angle) only. In significantly depolarizing layers the backscatter values should be corrected on the basis of climatological values for the depolarization ratio (desert dust, 20%; cirrus, 30%).

In the case of aerosol profiling in the lower troposphere based on 700 shot averages, the accuracy is also good under cloud–free conditions (Figure 5). Statistical errors of $<$20% can be reached even for the lidar ratio with 500 m signal resolution under bright background conditions. It should be emphasized that the simulated extinction coefficients (for 355 nm) of 100–150 Mm^{-1} represent very typical rather than extreme pollution conditions. Because of the dependence of the extinction error on $(\Delta z_\mathrm{j})^{-1.5}$, the uncertainty can be further reduced by almost a factor of 3 when the vertical signal resolution is changed from 500 to 1000 m. If the shot number is increased by a factor of 4, the statistical error is reduced by about a factor of 2.

The rather low vertical resolution results from the fact that the primary goal of ALADIN are wind observations and that wind observations with 500 m vertical resolution in the lower troposphere, 1000 m in the upper troposphere, and 2000 m in the stratosphere up to about 26–km height are sufficient. The limited resolution is also a consequence of the fact that the ALADIN detection unit (Accumulation CCD) can store information of 24 atmospheric layers only.

In conclusion, our study shows that ALADIN observations can be used to retrieve reliable results in terms of particle backscatter, extinction, and lidar ratio profiles. Global maps of aerosol and cloud optical properties obtained from ALADIN observations would thus be a valuable contribution to the long–term data record (2006–2014) provided by the CALIPSO, ADM–Aeolus, and EarthCARE missions.

REFERENCES

1. Stoffelen A., et al., The Atmospheric Dynamics Mission for global wind field measurement, *Bull. Amer. Meteor. Soc.*, 86, 73–87, 2005.

2. Endemann M., et al., The ADM–AEOLUS mission – The first wind lidar in space, Proc. 22nd ILRC, Italy, *ESA SP-561,* 2004

3. Eloranta E. W., High spectral resolution lidar, C. Weitkamp (Ed.), *LIDAR — Range–resolved optical remote sensing of the atmosphere*, *Springer*, New York, 2005.

4. Bruneau D., and Pelon J., Simultaneous measurements of particle backscattering and extinction and wind velocity by lidar with a Mach–Zehnder interferometer: principle of operation and performance assessment, *Appl. Opt.*, 42, 1101–1114, 2003.

5. Imaki M., and Kobayashi T., Ultraviolet high–spectral–resolution Doppler lidar for measuring wind field and aerosol optical properties, *Appl. Opt.*, 44, 6023–6030, 2005.

6. Ansmann A., and Müller D., Lidar and atmospheric aerosols, C. Weitkamp (Ed.), *LIDAR — Range–resolved optical remote sensing of the atmosphere*, *Springer*, New York, 2005.

7. Fernald F. G., Analysis of atmospheric lidar observations, *Appl. Opt.,* 23, 652–653, 1984.

8. Sasano Y., et al., Error caused by using a constant extinction/backscatter ratio in the lidar solution, *Appl. Opt.*, 24, 3929–3932, 1985.